Effect of pH Variation on Structural, Optical and Shape Morphology of BiVO 4 Photocatalysts

Conference Paper · December 2018

DOI: 10.1109/ICECE.2018.8636721

8 authors, including:

Manifa Noor
Bangladesh University of Engineering and Technology
11 PUBLICATIONS **1** CITATION
SEE PROFILE

Md. Abdullah Al Mamun
Bangladesh University of Engineering and Technology
11 PUBLICATIONS **1** CITATION
SEE PROFILE

Md Farabi Rahman
Bangladesh University of Engineering and Technology
16 PUBLICATIONS **9** CITATIONS
SEE PROFILE

Effect of pH Variation on Structural, Optical and Shape Morphology of $BiVO_4$ Photocatalysts

Manifa Noor, [1,*]M. A. Al Mamun, [1]M A Matin, [1] Md. Fakhrul Islam, [1]Saima Haque, [1]Farabi Rahman, [1]M. N. Hossain[1], M A Hakim[1]

[1]Department of Glass and Ceramic Engineering, Bangladesh University of Engineering and Technology
Dhaka 1000, Bangladesh
[*]rakin.manifa@gmail.com

Abstract—**Visible light driven photocatalysts have gathered enormous interest in recent years because of their capability to harvest energy directly from sunlight by water splitting and also to purify water. Bismuth Vanadate (BVO) is one of the most potential photocatalysts for water pollutant degradation and hydrogen production by oxidation of water. In our study, highly crystalline Bismuth Vanadate nanoparticles have been synthesized by a straightforward hydrothermal route where pH is varied to observe the change in morphology of the particles. Thermal analysis confirmed the tetragonal to monoclinic phase transformation temperature at 350 °C. A hierarchical development of monoclinic – tetragonal heterostructure of Bismuth Vanadate is further confirmed by Rietveld refinement of XRD patterns and the obtained particle size is 27nm. Band gap energy has been tailored through control of pH to explore the optical band gap for suitable photocatalytic properties. It is found that a heterostructure composed of rod and spherical shaped nanoparticles for a pH value 6.5, closer to neutral, demonstrating better optical properties for efficient photocatalytic activity with a band gap energy of 1.8 eV.**

Index Terms—**Bismuth Vanadate, hydrothermal, photocatalyst, Rietveld refinement**

I. Introduction

Energy requirement and reduction of environment pollution are the most concerning issues of the current world. The rapid growth of population all over the world demands more energy as well as pure water. Fossil fuels, the main source of energy, are destructive to the environment because of the Green House effect. Water pollution is also one of the most alarming subjects as the water level is rising due to Green House effect but the quantity of pure water is decreasing. So it is necessary to develop green technologies for energy production as well as the degradation of water pollutants. Capturing solar energy for energy production by H_2 generation from water splitting and degrading water pollutants by photochemical reaction can play a vital role to mitigate the energy and pure water crisis. When a photocatalyst absorbs sunlight, the photo excited electron goes from valence band to conduction band which in turns generates a pair of electron-hole and this electron-hole pair can oxidize or reduce other chemical compounds adhered to the photocatalysts' surface. This redox reaction can be utilized to produce H_2 energy by oxidation of water and to disintegrate water pollutants [1-6]. For this reason, the innovation of a photocatalyst with practical application has become a crying need to the researchers all over the world. Fujishima and Honda [17] discovered the water splitting phenomenon for the first time and since then the quest for developing such photocatalyst has remained still unsatisfied to the researchers. Several binary and ternary metal oxides have been developed such as TiO_2, Ag_3VO_4, $InNbO_4$, $InVO_4$, and $BiVO_4$. Among these oxides, $BiVO_4$ is considered as the most propitious candidate due to its non-toxicity and variable synthesis routes like sol-gel, co-precipitation, solid-state, hydrothermal, chemical bath deposition etc [8-12]. Park *et al.* reported that monoclinic scheelite phase ofBismuth Vanadate (m-$BiVO_4$) is a very promising photocatalyst with the ability to absorb a high amount of visible light[13]. But in most synthetic process, the synthesized nanoparticles have large crystal sizes and low surface areas [14-15]. Therefore, a search for developing m-$BiVO_4$ with large surface area and high photocatalytic activity is still going on.

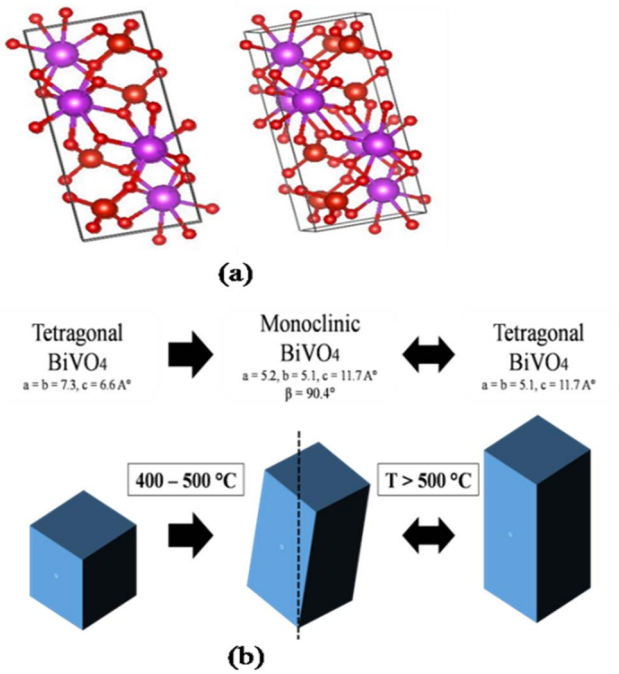

Fig 1: (a) Crystal structure of monoclinic $BiVO_4$ showing its 2 fold symmetry (b) Phase transformation with temperature

The natural source of $BiVO_4$ is pucherite which has orthorhombic crystal structure [16]. It is possible to synthesize scheelite and zircon type crystal structure of $BiVO_4$ in laboratory. Scheelite type structure can be both monoclinic and tetragonal while Zircon type structure contains tetragonal

978-1-5386-7482-6/18/$31.00©2018 IEEE.

phase only. The main difference between scheelite type tetragonal and zircon type tetragonal phase is in the lattice parameter. Scheelite structures consist of the Vanadium ions co-ordinated by four Oxygen atoms in tetrahedral sites and Bismuth ions coordinated by eight Oxygen atoms from eight different VO_4 tetrahedral units [17].

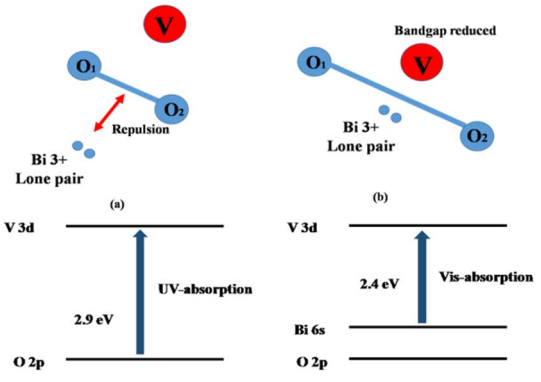

Fig 2: Schematic diagram of band gaps of (a) pure tetragonal zircon type BVO (b) pure monoclinic BVO

In tetragonal structure, all identical bonds are equal while distortion occurs in monoclinic structure. In tetragonal scheelite type BVO structure all V–O bond lengths are same (1.72A˚) while in monoclinic scheelite structure the V–O bond lengths are not equal (1.77 Å and 1.69 Å). Similarly, in tetragonal scheelite BVO structure, the two Bi–O distances are almost equal (2.453 Å and 2.499 Å) while the Bi–O bond lengths in the monoclinic scheelite structure are different (2.354 Å, 2.372 Å, 2.516 Å and 2.628Å) [18]. Since O–O bond length is higher in monoclinic structure than tetragonal structure, the repulsion between O 2p electrons and Bi^{3+} lone pair electrons decreases. So, band gap reduces in monoclinic structure. Fig 2 shows the graphical representation of the reduction of band gap in monoclinic BiVO4. Pure tetragonal $BiVO_4$ has band-gap energy of 2.9 eV while for monoclinic $BiVO_4$ the band-gap energy is 2.4 eV. However, to make $BiVO_4$ a better photocatalyst under visible light, its band gap should be further reduced and a heterostructure consisting of tetragonal and monoclinic phase can be a suitable solution in this regard.

In this experiment we have applied hydrothermal process for the synthesis of $BiVO_4$ using $Bi(NO_3)_3.5H_2O$, V_2O_5 and K_2SO_4 and pH was varied using $NaOH/HNO_3$ solution. Structural analysis, surface morphology, optical and thermal properties of the samples are carried out to predict their photocatalytic activity. The studies revealed the dependence of band gap with the change in pH which in turn affects the photocatalytic response of the synthesized particles.

II. Experimental

A. Synthesis of BVO nanoparticles

$BiVO_4$ nanoparticles were synthesized by following a hydrothermal route where $Bi(NO_3)_3.5H_2O$ and V_2O_5 were taken in a beaker with 1:1 molar ratio (0.2 mmol) as precursor. 10 mL of DI water was added along with K_2SO_4 (5.7 mmol) and the suspension was stirred for 5 minutes. Solutions of NaOH and HNO_3 were used for varying the pH of the solution and added drop-wise in the suspension very carefully. In a 25mL Teflon-lined Stainless Steel autoclave, the precursor suspension was taken and it was heated in a oven at 200 ºC for 24 hours and slowly cooled to room temperature. The precipitates were centrifuged at 4000 rpm for 5 minutes and dried subsequently. Finally the nanoparticles were collected and taken for further characterization. The parameters of the synthesis process are given in Table I.

Table I: Synthesis parameters of BVO nanoparticles

Sample ID	pH	Precursor	Molar amount (mmol)	Weight (mg)	Temp. (°C)
S1	2.5	$Bi(NO_3)_3.5H_2O$	0.2	97	200
S2	6.5	V_2O_5	0.2	36.38	
S3	9.5	K_2SO_4	5.7	1000	

B. Characterization of the synthesized nanoparticles

Structural analysis of the powder samples were carried out using X-Ray Diffraction Technique (Empyrean PANalytical-Netherlands) using CuKα radiation 1.54 Å. Crystallization temperature of the samples along with thermal kinetics were anticipated by Differential Scanning Calorimetry (DSC) and Thermo-gravimetric Analysis (TGA) at a heating rate 10ºC/min from room temperature upto 800 ºC (NETZSCH, STA 449 F3 Jupiter). The surface morphology of the powder samples were observed by Field Emission Scanning Electron Microscope (JSM, 7600 Jeol). Optical properties of the samples were measured by using a UV-Vis spectrometer (UV/Vis/NIR – Lambda 1050, PerkinElmer, USA).

III. Results and Discussions

Fig 3 (a – c) shows the DSC and TGA graphs of the synthesized nanoparticles.

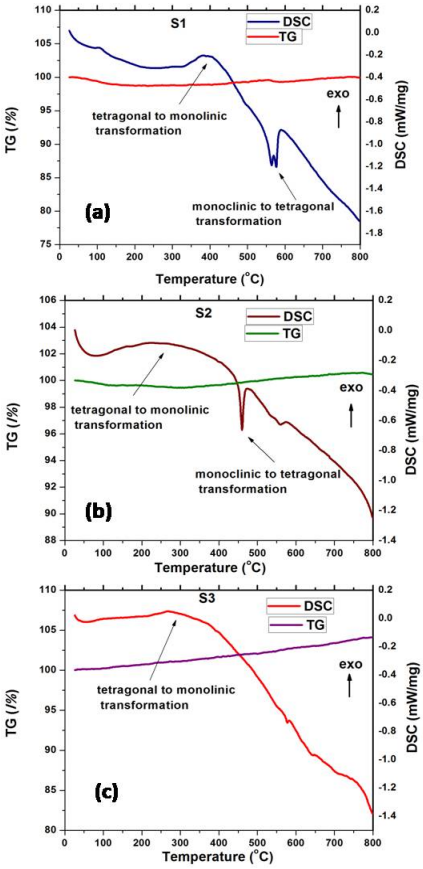

Fig 3: DSC and TGA graphs of (a) S1, (b) S2 and (c) S3

From the DSC results of S1 and S2 it is seen that an exothermic reaction occurs at ~350 ºC which indicates tetragonal to monoclinic transformation. An endothermic peak is observed above 400 ºC for both S1 and S2 which is attributed to the monoclinic to tetragonal reversible transformation. In case of S3, above 250 ºC tetragonal to monoclinic transformation occurs but no significant monoclinic to tetragonal transformation is observed. So, for the higher value of pH, the reversible monoclinic to tetragonal transformation at higher temperature is suppressed. No significant weight loss occurs due to the crystallographic phase transformation which is indicated by the TG curves.

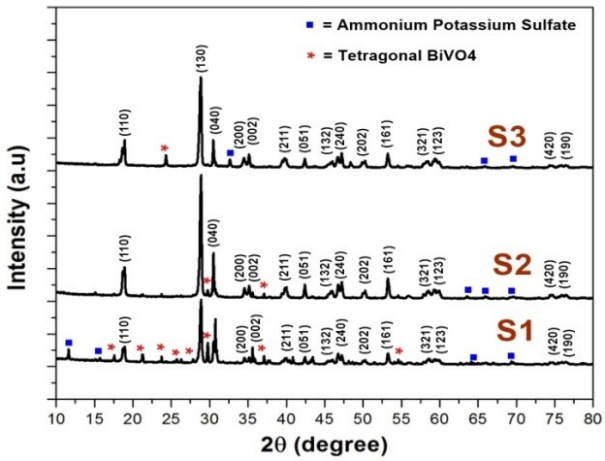

Fig 4: PXRD patterns of S1, S2 and S3 showing monoclinic BVO phase, tetragonal BVO phase and Ammonium Potassium Sulphate phase

Fig 4 shows the PXRD patterns of all the synthesized samples. From the XRD patterns it is visible that at 2θ values 18.5°, 35° and 46° peak splitting occurred which matched completely with Scheelite type monoclinic $BiVO_4$ phase (ICSD 98-010-0604). Some tetragonal $BiVO_4$ phase is also present (ICDD 01-074-4892) which gradually decreased with the increase in pH. At 2θ = 17.5°, 30°, 37.5° the suppression of peak intensity of tetragonal phase is observed with the increase in pH. Some impurity phase appeared as Ammonium Potassium sulphate that couldn't be removed even after centrifuging for several times. The crystallite size of monoclinic phase is calculated by using Scherrer Formula-

$$D = \frac{k\lambda}{\beta cos\theta} \qquad (1)$$

where D is the crystallite size (nm), β is the full width half maximum for (130) plane (rad), θ is the Bragg angle (deg), k is 0.9 (assuming spherical shape) and λ is 1.54Å. The amount of tetragonal and monoclinic phase along with the crystallite size is given in Table II.

Table II: Percentage of Phases and Crystallite Size

Sample ID	Monoclinic $BiVO_4$ ICSD 98-010-0604	Tetragonal $BiVO_4$ ICDD 01-074-4892	Ammonium Potassium Sulphate ICDD 01-087-2359	Crystallite Size (nm)
S1	26 %	68 %	6 %	27
S2	62 %	22 %	16 %	27
S3	81 %	13 %	6 %	27

Optical properties of the samples are investigated from the Diffused Reflectance spectra shown in Fig 5(a). Optical band gap energy of the samples are calculated using Kubelka – Munk function [19]

$$F(R) = \frac{(1-R)^2}{2R} \qquad (2)$$

where R is the diffused reflectance of the samples. Plotting photon energy $(h\vartheta)$ vs $[F(R)h\vartheta]^{\frac{1}{n}}$ where n is 2 for indirect band gap and 1/2 for direct band gap.

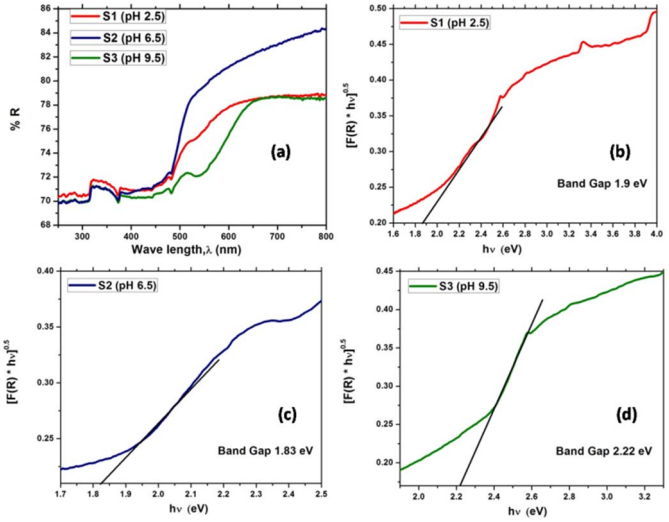

Fig 5: (a) Diffused reflectance spectra of samples; Optical band-gaps of (b) S1 (c) S2 and (d) S3

For our samples we found sharp fall of the graph for n=2 which indicates that all of our samples have indirect band gap. The intersection of the slope of the graph with X-axis indicates the band gap of a particular sample. From Fig. 5 (b – d) it is visible that the obtained band gap energy of the samples S1(pH 2.5), S2(pH 6.5) and S3(pH 9.5) are 1.9eV, 1.83 eV and 2.22 eV respectively. So, with the increase in pH, band gap decreases at first up to a neutral pH 6.5 (S2) and then with further increase in pH, the band gap decreases (S3). Since S2 shows lowest band gap 1.8 3eV and the visible light energy range is 1.8-3.1 eV, the lowest energy photons of visible light are capable of transferring charge from valance band to conduction band. So the sample S2 with pH 6.5 is the best photocatalyst under visible light.

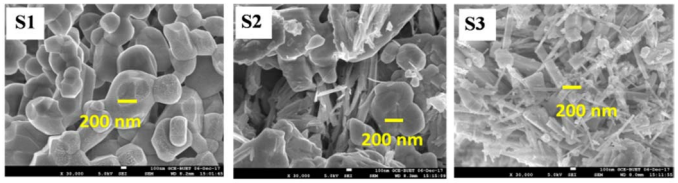

Fig 6 (a): FESEM images of S1, S2 and S3 taken at 5.00 kV (Magnification x30,000)

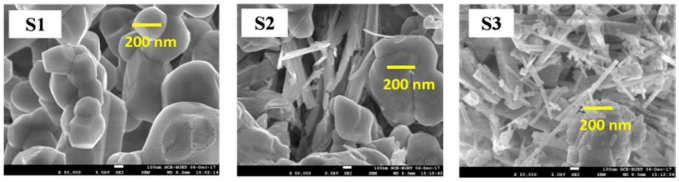

Fig.6 (b): FESEM images of S1, S2 and S3 taken at 5.00 kV (Magnification x50,000)

Shape morphology of the synthesized particles are shown in the FESEM images (Fig 6).It is clearly visible from the FESEM images that for lower pH (S1) the particles are of spherical shape and for higher pH (S3) rod shape appeared. For the neutral pH (S2, pH 6.5) a heterostructure containing rod and spherical shape has been formed. This sample S2 with 62% monoclinic BVO phase and 22% tetragonal phase is expected to show better photocatalytic property than the rest which is further supported by the optical properties of the sample.

IV. Conclusions

In this report, we have showed that in the presence of inorganic morphology controlling agent (K_2SO_4), pure m-$BiVO_4$ can be synthesized in a straightforward hydrothermal process. The average crystallite size of the samples calculated from XRD analysis is 27nm. Difference in surface morphology with pH variation is clearly visible in the SEM images which indicated spherical and combination of rod and spherical shaped particles. Optimization of the band gap energy has been established through control of pH value of the precursor suspension. A lower value of band gap 1.83eV has been obtained for S2 with a pH value of 6.5 along with a heterostructure of rod and spherical shape. This unique lower value of band gap energy as well as heterostructure of the synthesized BVO photocatalyst surface would facilitate the absorption of larger portion of visible light spectrum and enhance its photocatalytic activity. It is suggested that photocatalytic experiment needs to be carried out in much details to investigate the performance of the synthesized nanoparticles with various pH.

Acknowledgement

The authors acknowledge the support of the Department of Glass and Ceramic Engineering, BUET for providing the “Nano synthesis Laboratory” and characterization facilities.

References

[1] S.H.S. Chan, T.Y. Wu, J.C. Juan, C.Y. Teh, Recent developments of metal oxide semiconductors as photocatalysts in advanced oxidation processes (AOPs) for treatment of dye waste-water , J. Chem. Tech. Biotech., 86 (2011), pp. 1130-1158

[2] A.B. Djurišić, Y.H. Leung and A.M.C. Ng, Strategies for improving the efficiency of semiconductor metal oxide photocatalysis, Mater. Horiz., 1 (2014), pp. 400-410

[3] E. Pelizzetti and C. Minero, Metal oxides as photocatalysts for environmental detoxification, Comments Inorg. Chem., 15 (1994), pp. 297-337

[4] T. Hisatomi, J. Kubota and K. Domen, Recent advances in semiconductors for photocatalytic and photoelectrochemical water splitting, Chem. Soc. Rev., 43 (2014), pp. 7520-7535

[5] M.R. Hoffmann, S.T. Martin, W. Choi and D.W. Bahnemann, Environmental applications of semiconductor photocatalysis, Chem. Rev., 95 (1995), pp. 69-96

[6] Aracely Hernández-Ramírez and Iliana Medina-Ramírez, Photocatalytic Semiconductors, Springer, 2015, ISBN 978-3-319-10998-5.

[7] A. Fujishima and K. Honda, Electrochemical photolysis of water at a semiconductor electrode, Nature, 1972, 238 (5358): 37-8.

[8] A. Kudo, K. Ueda, H. Kato and I. Mikami, Photocatalytic O2 evolution under visible light irradiation on BiVO4 in aqueous AgNO3 solution. Catalysis Letters, 1998, vol. 53, p.229.

[9] H. Liu, R. Nakamura and Y. Nakato, Promoted photo-oxidation reactivity of particulate BiVO4 photocatalyst prepared by a photo assisted sol-gel method, Journal of Electrochemical Society, 2005, 152, G856.

[10] S. Tokunaga, H. Kato and A. Kudo, Selective Preparation of Monoclinic and Tetragonal BiVO4 with Scheelite Structure and Their Photocatalytic Properties, Chemistry of Materials, 2001, 13, p. 4624.

[11] J. B. Liu, H. Wang, S. Wang and H. Yan, Hydrothermal preparation of BiVO4 powders, Materials Science and Engineering: B, Volume 104, Issues 1–2, 15 November 2003, p.36–39.

[12] F. Rullens, A. Laschewsky and M. Devillers, Bulk and thin films of bismuth vanadates prepared from hybrid materials made from an organic polymer and inorganic salts, Chem. Mater., 2006, 18, p.771.

[13] Y. Park, K.J. McDonald and K.S. Choi, Progress in bismuth vanadate photoanodes for use in solar water oxidation, Chem. Soc. Rev.,2013, vol.42, pp.2321−2337.

[14] L. Zhou, W.Z. Wang, S.W. Liu, L.S. Zhang, H.L. Xu and W. Zhu, A sonochemical route to visible-light-driven high-activity BiVO4 photocatalyst, Journal of Mol. Catal. A: Chem. 252 (2006) .pp.120–124.

[15] H.Q. Jiang, H. Endo, H. Natori, M. Naga and K. Kobayashi, Fabrication and photoactivities of spherical shaped BiVO4 photocatalysts through solution combustion synthesis method ,J. Eur. Ceram. Soc. 28 (2008), pp. 2955–2962.

[16] T. Kako and J. Ye, Mater, Comparison of photocatalytic activities of two kinds of lead magnesium niobate for decomposition of organic compounds under visible-light irradiation, Trans, 2005, vol. 46, p.2694

[17] A. Kudo, K. Omori and H. Kato, A Novel Aqueous Process for Preparation of Crystal Form-Controlled and Highly Crystalline BiVO4 Powder from Layered Vanadates at Room Temperature and Its Photocatalytic and Photophysical Properties , J. Am. Chem. Soc. ,1999, vol.121, pp 11459–11467.

[18] A.W. Sleight, H.Y. Chen and A. Ferretti, Control of crystal phase of BiVO4 nanoparticles synthesized by microwave assisted method, Mater. Res. Bull.,1979, vol. 14, pp.1571–1581.

[19] P. Kubelka and F. Munk, EinBeitragZurOptik Der Farbanstriche, ZeitschriftfürTechnischePhysik, 1931, vol.12, pp.593-601.